Quantitative Analysis of the Isolated GAAA Tetraloop/Receptor Interaction in Solution: A Site-Directed Spin Labeling Study†

Peter Z. Qin,‡,§ Samuel E. Butcher,§,|| Juli Feigon,§ and Wayne L. Hubbell*,‡,§

Jules Stein Eye Institute and Department of Chemistry and Biochemistry, University of California, Los Angeles, California 90095

Received February 12, 2001; Revised Manuscript Received April 18, 2001

ABSTRACT: The GNRA (N: any nucleotide; R: purine) tetraloop/receptor interaction is believed to be one of the most frequently occurring tertiary interaction motifs in RNAs, but an isolated tetraloop/receptor complex has not been identified in solution. In the present work, site-directed spin labeling is applied to detect tetraloop/receptor complex formation and estimate the free energy of interaction. For this purpose, the GAAA tetraloop/receptor interaction was chosen as a model system. A method was developed to place nitroxide labels at specific backbone locations in an RNA hairpin containing the GAAA tetraloop. Formation of the tetraloop/receptor complex was monitored through changes in the rotational correlation time of the tetraloop and the attached nitroxide. Results show that a hairpin containing the GAAA tetraloop forms a complex with an RNA containing the 11-nucleotide GAAA tetraloop receptor motif with an apparent K_d that is strongly dependent on Mg^{2+}. At 125 mM $MgCl_2$, $K_d = 0.40 \pm 0.05$ mM. The corresponding standard free energy of complex formation is −4.6 kcal/mol, representing the energetics of the tetraloop/receptor interaction in the absence of other tertiary constraints. The experimental strategy presented here should have broad utility in quantifying weak interactions that would otherwise be undetectable, for both nucleic acids and nucleic acid−protein complexes.

Specific interaction between a GNRA[1] hairpin loop and the asymmetric internal loop called the tetraloop receptor facilitates long-range tertiary interactions in large RNA molecules (*1*−*4*). Among the limited number of RNA tertiary interaction modules known today (*5*), the GNRA tetraloop/receptor interaction was the first one to be identified, and is believed to be one of the most frequently occurring motifs in RNA (*3*, *4*, *6*). Recently, the GAAA tetraloop/receptor pair, the best known member of the GNRA tetraloop/receptor family, was utilized to engineer new RNA tertiary contacts for many applications, such as facilitating RNA crystallization and creating novel RNA nano-structures (*7*, *8*).

Various studies have revealed the functional importance and energetics of the GNRA tetraloop/receptor interaction embedded within various RNA molecules (*1*−*3*, *8*−*14*). An important conclusion from these studies is that tertiary interactions in RNAs are thermodynamically coupled, and the energetic contribution of the tetraloop/receptor interaction strongly depends on the presence of other RNA interaction elements (*8*, *14*). However, it has not been possible to measure the basal energetics of the tetraloop/receptor interaction in isolation, because the isolated complex has not been observed in solution. Without such a basal value, it is difficult to dissect energetic contributions of different RNA interaction elements and to study their roles in RNA tertiary folding.

Elucidation of the detailed pathway of complex formation is an important aspect in the study of the tetraloop/receptor motif (*15*). Some clues regarding possible pathways have come from structural studies of isolated tetraloops and receptors (*16*, *17*), and tetraloop/receptor complexes in crystals (*18*, *19*). Based on the structural similarity of GNRA tetraloops in solution and in the crystalline complex (*16*, *18*, *19*), and on the large conformational difference between the GNRA tetraloop receptor free in solution and in the crystalline complex (Figure 1A) (*17*, *18*), a specific model for the pathway of complex formation has been proposed (*17*). To evaluate such models, it would be of great advantage to have a technique and proper experimental conditions to observe the formation of an isolated tetraloop/receptor complex in solution.

Here, site-directed spin labeling (SDSL) is employed to quantitatively investigate the strength of the isolated GNRA tetraloop/receptor interaction. The general strategy of SDSL is to introduce a nitroxide probe that contains a stable, unpaired electron at a selected site in the macromolecule and

† The research reported here was supported by NIH Grant EYO5216 (W.L.H.), the Jules Stein Professor Endowment (W.L.H.), Bruce Ford Bundy and Anne Smith Bundy Foundation (W.L.H.), NSF Grant MCB-9808072 (J.F.), and NIH Grant R01 GM 37254 (J.F.). P.Z.Q. is a DuPont Pharmaceutical Fellow of the Life Sciences Research Foundation.

* To whom correspondence should be addressed at the Jules Stein Eye Institute, UCLA School of Medicine, 100 Stein Plaza, Los Angeles, CA 90095-7008. Tel: (310) 206-8830; Fax: (310) 794-2144; Email: hubbellw@jsei.ucla.edu.

‡ Jules Stein Eye Institute.

§ Department of Chemistry and Biochemistry.

|| Current address: Department of Biochemistry, 433 Babcock Dr., University of Wisconsin−Madison, Madison, WI 53706.

[1] Abbreviations: GNRA, N, any nucleotide, R, purine; SDSL, site-directed spin labeling; EPR, electron paramagnetic resonance; MES, 2-(*N*-morpholino)ethanesulfonic acid; MOPS, 3-(*N*-morpholino)propanesulfonic acid; Tris, 2-amino-2-(hydroxymethyl)-1,3-propanediol.

10.1021/bi010294g CCC: $20.00
Published on Web 05/16/2001

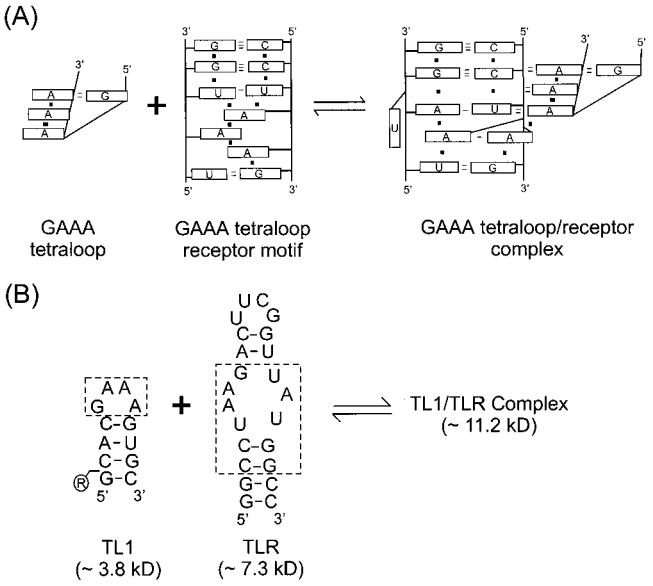

FIGURE 1: Formation of the GAAA tetraloop/receptor complex. (A) Schematics of structures of the isolated GAAA tetraloop and receptor in solution (*16*, *17*) and that of a GAAA tetraloop/receptor complex observed in the crystal of the P46 domain of the group I intron *Tetrahymena* (*18*). (B) The sequence of the GAAA tetraloop hairpin (TL1) is shown, with R indicating the nitroxide labeling site. Also shown is the TLR RNA, which has the 11-nucleotide GAAA tetraloop receptor embedded (indicated by the dashed box). Molecular masses for the corresponding molecules are indicated.

interpret the EPR spectrum of the labeled molecule in terms of structure and dynamics (*20*−*23*). Three fundamental types of information are obtained from the EPR spectrum of a nitroxide in a native macromolecule: (1) the dynamics of the nitroxide; (2) the accessibility of the nitroxide to collision with a paramagnetic reagent in solution, essentially the solvent accessibility; and (3) the distance of the nitroxide from a second nitroxide or a bound metal ion. During the past decade, SDSL has been developed and successfully applied to the study of the structure, dynamics, and interaction of a variety of proteins, especially membrane and membrane-associated proteins, that are difficult to study by conventional methods such as X-ray crystallography and NMR spectroscopy. The spin labeling technique has also been applied to studies of nucleic acids, although these reports primarily focused on DNA (*24*). Recently, several groups reported methods to site-specifically attach spin labels to RNA molecules (*25*−*27*). However, exploration of the potential of SDSL for studying structure, dynamics, and function of RNA has just begun (*24*).

In this study, the GAAA tetraloop was used as a representative GNRA tetraloop, and complex formation was studied with its 11-nucleotide receptor (Figure 1). A method was developed to attach a nitroxide to an RNA hairpin containing the GAAA tetraloop. EPR spectroscopy was used to monitor changes in rotational correlation time (τ) of the labeled RNA, which reflects the formation of the tetraloop/receptor complex due to increase in molecular size (Figure 1B). The results reveal that, in the presence of magnesium ions, the GAAA tetraloop and receptor interact specifically in the absence of other RNA elements, with a dissociation constant in the 10^{-4} M range. The free energy of formation of the isolated tetraloop/receptor interaction is −4.6 kcal/mol, which likely represents the basal contribution of the interaction.

MATERIALS AND METHODS

RNA Synthesis. The GAAA tetraloop hairpin RNA, designated TL0, has the sequence 5′GCACGAAAGUGC, where the GAAA tetraloop sequence is underlined. A modified RNA, designated TL1, has the sequence 5′G_{ds}CACGAAAGUGC, where ds represents a deoxyribo−phosphorothioate linkage between the first and second nucleotides. The substitution of the 2′-OH group by a 2′-H group is necessary to prevent strand scission upon labeling of the phosphorothioate linkage (*28*, *29*). The mTL RNA has the sequence 5′G_{ds}CACUUCGGUGC, where the UUCG tetraloop sequence is underlined. TL0, TL1, and mTL were synthesized by Dharmacon, Inc. (Lafayette, CO). After deprotecting the 2′-OH groups following procedures provided by the vendor, RNA was purified through anion exchange HPLC using a PA100 column (4 × 250 mm) (Dionex Inc., Sunnyville, CA), eluted with a gradient formed by mixing buffer A (1 mM $NaClO_4$, 20 mM Tris-HCl, pH 6.8, and 20% acetonitrile) and buffer B (400 mM $NaClO_4$, 20 mM Tris-HCl, pH 6.8, and 20% acetonitrile). The flow rate was 2.0 mL/min, and the gradient was 0−12% B in 2 min, followed by 12−17% B in 13 min. Elution of the RNA was monitored by absorbance at 260 nm. Fractions containing RNA were desalted using Oligonucleotide Purification Cartridges (OPC, Applied Biosystems Division, Perkin-Elmer, Foster City, CA) following the procedure provided by the vendor. To minimize loss of the RNA due to its small size, the washing step was modified to 10 mL of 50 mM triethylamine acetate instead of 10 mL of water. The desalted RNA was eluted from the OPC column with 1 mL of 50% (v/v) acetonitrile/water, lyophilized to dryness, resuspended in water, and stored at −20 °C. The resulting RNA migrated as a single band when visualized on a 20% denaturing polyacrylamide gel.

The GAAA tetraloop receptor RNA, designated TLR, was synthesized and purified as described (*17*). The stock solution of TLR was 1 mM and pH 6.2. Concentrations of RNA oligonucleotides were determined by UV absorbance at 260 nm using an extinction coefficient of 141 193 cm^{-1} M^{-1} for TL1 and 248 966 cm^{-1} M^{-1} for TLR, respectively.

Spin Labeling of the Modified RNA. Thiol-reactive nitroxide derivative, 3-iodomethyl-(1-oxy-2,2,5,5-tetramethylpyrroline) (reagent **V**, Figure 2A), was prepared from a precursor, 1-oxyl-2,2,5,5-tetramethyl-3-methane-sulfonyloxymethylpyrroline (kindly provided by Dr. K. Hideg, University of Pécs, Hungary), following a published procedure (*30*). Briefly, the precursor (5−10 mM) was mixed with an equal molar amount of NaI in acetone. After incubating the mixture at 37 °C for 30−60 min, the precipitant was removed by filtration and the solvent removed under vacuum to yield **V** as a red oil. The product was used without further purification.

Labeling of TL1 was carried out in a reaction mixture containing 10% (v/v) 1.0 M MES, pH 5.8, 50% (v/v) formamide, and 60−100 mM freshly prepared **V**. The RNA concentration was 0.1−1 mM. The reaction was carried out at room temperature for 12−16 h with constant shaking. The labeled RNA was purified by anion exchange HPLC, following the procedure described above.

Measurement of RNA Melting Temperature. Thermal denaturation of TL0 and nitroxide-labeled TL1 RNA was carried out in a Cary 100 UV−Vis spectrophotometer

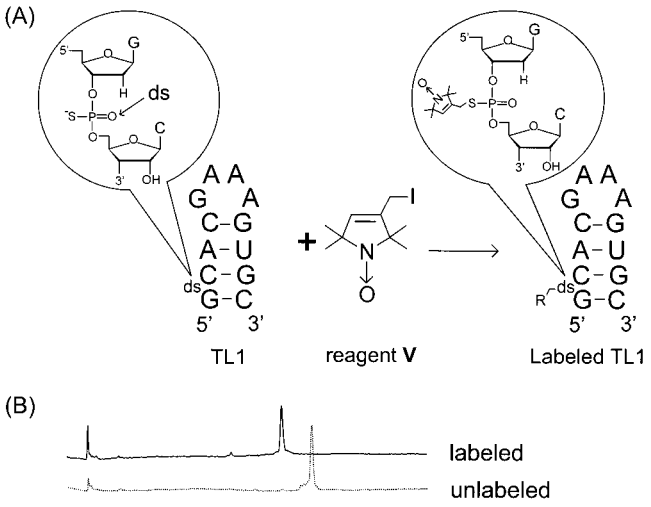

FIGURE 2: Spin labeling of the TL1 RNA hairpin with reagent **V**. (A) Schematic representation of the RNA labeling reaction, where ds represents the deoxyribo−phosphorothiolate linkage and R represents the attached nitroxide group. (B) Elution profile of anion exchange HPLC of TL1 RNA hairpins monitored by the 260 nm absorbance (Materials and Methods).

(Varian Instruments, Walnut Creek, CA). RNA samples were ∼0.3 AU at 260 nm (20 °C) in 50 mM phosphate buffer (pH 7.0) and 100 mM NaCl. The temperature was ramped at a speed of 0.5 °C/min from 35 to 95 °C, and data were collected at 30 s intervals. Derivatives of the absorbance data were calculated, and the melting temperatures (T_m) were determined from the maximum of the first derivative.

EPR Measurements. EPR spectra were acquired under field frequency lock in a Varian E-109 spectrometer fitted with a two-loop one-gap resonator (*31*). Samples of 4 μL were loaded in 0.84 mm o.d. capillaries (VitroCom Inc., Mountain Lakes, NJ) that were sealed on one end. All spectra were acquired at X-band using a 2 mW incident microwave power and a 100 G scan width. The 100 kHz field modulation amplitude and time constant of the detector were optimized to provide maximum signal-to-noise ratio with no line broadening. For comparison, the spectra were normalized with respect to the total number of spins. Acquisition and manipulation of EPR spectra were carried out using computer programs written in LabVIEW (National Instruments, Austin, TX) by Dr. C. Altenbach.

The effective rotational correlation time, τ, of the nitroxide was estimated as (*32*):

$$\tau\,(\mathrm{s}) = (6.5 \times 10^{-10})\Delta H_0\left(\sqrt{\frac{h(0)}{h(-1)}} - 1\right) \qquad (1)$$

where ΔH_0 is the peak-to-peak line width of the central line in Gauss and $h(0)$ and $h(-1)$ are the peak-to-peak amplitudes of the central and high-field lines, respectively (Figure 3, inset). It should be noted that eq 1 was derived for homogeneously broadened spectra (*32*−*34*). Corrections due to inhomogeneous broadening were determined to be ≤±5% according to procedures described by Bales (*35*).

Analysis of Binding between the GAAA Tetraloop and Its Receptor. Binding experiments were carried out with a fixed concentration of labeled TL1 (∼30 μM) and various concentrations of TLR (0−1.75 mM). For each measurement, the desired amount of TLR was lyophilized to dryness, and

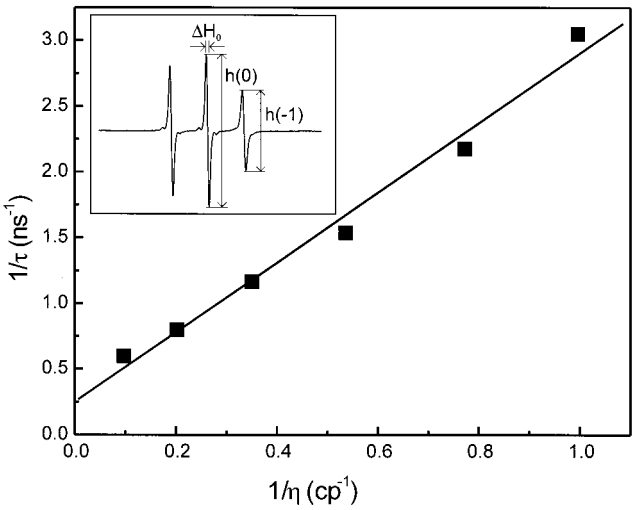

FIGURE 3: Viscosity dependence of the rotational correlation time of spin labeled TL1 RNA hairpin. Experiments were carried out at 20 °C in a solution containing 50 mM phosphate buffer (pH 7.0), 100 mM NaCl, and ∼30 μM labeled TL1, with various amounts (0−50%, w/v) of sucrose. The corresponding viscosities were obtained from (*53*), and τ was determined according to eq 1. Data were fitted to eq 5 to determine $\tau_R^{\mathrm{tetraloop}} = 0.38 \pm 0.02$ ns and $\tau_i = 4.0 \pm 1.6$ ns. Inset: EPR spectrum of labeled GAAA tetraloop hairpin (TL1) in 100 mM NaCl, 50 mM phosphate (pH 7.0) in the absence of added sucrose. ΔH_0 presents the peak-to-peak line width of the central line in Gauss, and $h(0)$ and $h(-1)$ are the peak-to-peak amplitudes of the central and high-field lines, respectively.

4 μL of a solution containing labeled TL1 and the desired concentrations of $MgCl_2$, NaCl, and KCl was added. Preheating the RNAs at 95 °C and annealing at room temperature or on ice under various lengths of time had no effects on the measurements. The pH of the mixture was measured to be ∼6.0. No significant variation in pH was found when the RNA concentration was varied in these experiments. EPR spectra were recorded as described.

The resulting first-derivative EPR spectra were analyzed in terms of two components, one arising from free (unbound) TL1 in solution and the other from TL1 in the complex. The spectrum of the complexed TL1 was extracted by a spectral titration procedure as outlined by Griffith and colleagues (*36*). Briefly, the composite spectrum was titrated by incrementally subtracting the free TL1 spectrum until oversubtraction occurred (as indicated by phase reversal within part of the resulting spectrum). The final endpoint of the titration was determined by the appearance of a well-behaved first integral with no negative excursions below the baseline. The ratio of double integrals corresponding to the free and complexed spectra then represents the ratio of free and complexed TL1 populations. The apparent dissociation constant (K_d) was determined by fitting a plot of the fraction of free population (f_{free}) versus the concentration of the TLR ([TLR]) to the binding isotherm:

$$f_{\mathrm{free}} = \frac{K_d}{[\mathrm{TLR}] + K_d} \qquad (2)$$

To examine the salt dependence of binding, EPR spectra were obtained in 50 mM phosphate buffer (pH 6.0) following the procedures described above with either 500 mM NaCl, 500 mM KCl, or 125 mM $MgCl_2$.

To further quantitate the Mg^{2+} dependence, complex formation was measured in various concentrations of $MgCl_2$ in the presence of 100 mM NaCl and 50 mM MOPS (pH 6.6), with labeled TL1 at ~30 μM and TLR at 1 mM. The experimental values of f_{free} were plotted against the concentration of Mg^{2+}, and the data were fitted to the following isotherm to obtain the apparent dissociation constant for Mg^{2+} (K_{mg}):

$$f_{free} = \frac{K_{mg}}{[Mg^{2+}] + K_{mg}} \quad (3)$$

RESULTS

Spin Labeling of the GAAA Tetraloop Hairpin. To provide a reactive functionality for the attachment of a nitroxide spin label within the RNA hairpin, a phosphorothioate linkage was introduced near the 5′ terminus of the TL1 hairpin (Figure 2A) (Materials and Methods). During anion exchange purification, the phosphorothioate-modified RNA eluted later than the unmodified RNA, consistent with previous reports (*37*). Interestingly, the modified RNA itself resolved into two closely eluting components. On a 20% denaturing polyacrylamide gel, both fractions of the modified RNA showed a mobility similar to that of the unmodified RNA, indicating that they were both full-length, intact RNA. Both fractions reacted with the nitroxide probe **V** with similar efficiency and gave identical EPR spectra (as in Figure 3, inset). It is likely that the two fractions represent isomers of the modified phosphorothioate group introduced during chemical synthesis (*37*). Because the modification site is far away from the GAAA tetraloop, the two isomers should be identical with respect to the tetraloop/receptor interaction. Therefore, the identities of the two modified RNA fractions were not further characterized. The late-eluting RNA fraction was used in all of the following experiments and is designated TL1.

The efficiency of RNA labeling was quantified using anion-exchange HPLC (Figure 2B). The labeled RNA eluted earlier than the phosphorothioate derivative, which is consistent with the loss of a negative charge upon labeling. The labeling efficiency was close to 100%, and no degradation of RNA was observed during the reaction. The melting temperature of the labeled RNA was determined to be 64.5 ± 1.0 °C, very similar to that of the unmodified TL0 RNA (68.0 ± 1.0 °C). This indicates that the presence of the nitroxide label does not severely perturb the RNA secondary structure.

EPR Spectra of the GAAA Tetraloop Hairpin. The EPR spectrum of labeled TL1 in aqueous solution at ambient temperature consists of three sharp lines (Figure 3, inset), characteristic of a nitroxide undergoing rapid isotropic rotation. The effective correlation time (τ) for rotational diffusion of the nitroxide group, estimated according to eq 1, is 0.33 ns.

The effective correlation time has contributions from the rotational diffusion of the RNA hairpin in solution, with a characteristic correlation time τ_R, and from internal modes, such as rotation about the bonds that connect the nitroxide to the backbone, which can be represented by a net effective correlation time τ_i. Assuming that the overall rotational diffusion and internal modes are independent and isotropic, τ can be expressed as:

$$\frac{1}{\tau} = \frac{1}{\tau_i} + \frac{1}{\tau_R} \quad (4)$$

The rotational correlation time τ_R is taken to be directly proportional to the viscosity of the solution. However, τ_i is apparently independent of viscosity for concentrations of sucrose less than about 40% w/v, because bond rotational rates are determined by internal potentials rather than the solution viscosity (*38, 39*). With these assumptions, eq 4 can be written as:

$$\frac{1}{\tau} = \frac{1}{\tau_i} + \frac{1}{\tau_R^{tetraloop}} \times \frac{1}{\eta} \quad (5)$$

where η is the viscosity coefficient and $\tau_R^{tetraloop}$ represents the measured rotational correlation time of labeled TL1 in water ($\eta \cong 1$ cP). Equation 5 predicts a linear relationship between $1/\tau$ and $1/\eta$. To test this, the solution viscosity was varied at a fixed temperature by addition of various amounts of sucrose. As shown in Figure 3, a plot of $1/\tau$ vs $1/\eta$ is linear within experimental error. From a fit of the data to eq 5 (solid trace), $\tau_R^{tetraloop}$ was determined to be 0.38 ± 0.02 ns (from the slope), and τ_i was determined to be 4.0 ± 1.6 ns (from the *y*-intercept). The observed correlation time τ is clearly dominated by the faster rotational diffusion rate of the tetraloop hairpin.

Detection of GAAA Tetraloop/Receptor Complex in Solution. The molecular mass of the tetraloop/receptor complex (TL1/TLR) is estimated to be ~11 kDa, which is approximately 3 times larger than that of the tetraloop hairpin (TL1, Figure 1B). Because τ_R is proportional to molecular size and hence approximately proportional to molecular mass, the tetraloop/receptor complex is expected to have a longer τ_R. The observed correlation time of the nitroxide is dominated by τ_R, and complex formation is expected to produce an increase in the observed correlation time. As shown in Figure 4A, addition of 1.75 mM TLR to labeled TL1 does in fact lead to changes in the EPR spectrum consistent with an increase in correlation time, i.e., a broadening in both high-field and low-field lines with a concomitant reduction in amplitude.

While the change in τ is consistent with an increase in τ_R due to increase of molecular mass upon formation of the tetraloop/receptor complex, it might also arise from other sources, such as viscosity changes in the solution upon addition of a large amount of receptor RNA oligonucleotide. Alternatively, changes in the EPR spectrum might just reflect nonspecific RNA interactions from the high concentration of RNA oligonucleotides used in the experiment. To test for these possibilities, the GAAA tetraloop in the TL1 RNA oligonucleotide was mutated to a UUCG tetraloop (mTL), which does not bind specifically with the GAAA tetraloop receptor (*1*). Under the same conditions used in the TL1 experiments, addition of 1.75 mM TLR to the labeled mTL led to much smaller changes in the observed EPR spectrum (Figure 4B, vide infra). This verifies that the observed changes in the EPR spectra of TL1 upon addition of TLR are due to the specific interaction between the GAAA tetraloop and its receptor. Therefore, the increase in correla-

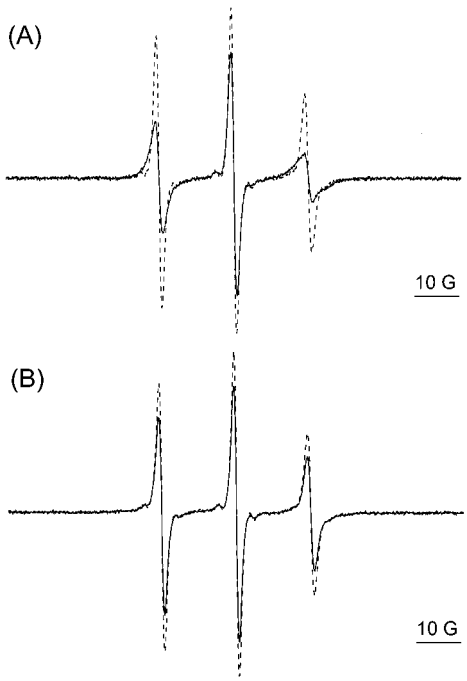

FIGURE 4: Detecting the tetraloop/receptor complex in solution. (A) Superimposed EPR spectra of labeled TL1 in the absence (dashed trace) and presence of 1.75 mM receptor TLR (solid trace). Spectra were obtained in 125 mM $MgCl_2$, 500 mM NaCl, and 500 mM KCl. The pH is 6.0. (B) Superimposed EPR spectra of a nitroxide labeled RNA containing a UUCG tetraloop in the absence (dashed trace) and presence of 1.75 mM GAAA tetraloop receptor TLR (solid trace). Buffer conditions are the same as those in (A).

tion time of the nitroxide in labeled TL1 serves as an indicator for the specific GAAA tetraloop/receptor interaction.

Quantification of Tetraloop/Receptor Interaction. The EPR spectrum in the presence of receptor reveals two components corresponding to spin populations with different correlation times (Figure 5A and inset, solid trace). Presumably, these populations correspond to a tetraloop/receptor complex and free tetraloop in slow exchange on the EPR time scale. Consistent with this assumption, the relative amounts of the two components changed when the amount of receptor was varied at a fixed tetraloop concentration.

To quantitatively analyze the tetraloop/receptor interaction, the two components were resolved by subtraction of the spectrum of TL1 alone from the composite spectrum using the spectral titration procedure described under Materials and Methods. A representative set of spectra for an equilibrium mixture containing 1.75 mM TLR and ~30 μM labeled TL1 is shown in Figure 5A. Interestingly, the result for the tetraloop/receptor complex (Figure 5B, solid trace) can be simulated using a model of a nitroxide undergoing an axially symmetric anisotropic rotational diffusion (Figure 5B, dashed trace) (*40, 41*), with $R_{||} = 4.85 \times 10^8$ s^{-1} and $R_{\perp} = 6.40 \times 10^7$ s^{-1}, where $R_{||}$ and $R_{\perp}$ are the corresponding elements of the rotational diffusion tensor.

The relative concentrations of bound (complexed) and free TL1 in equilibrium are provided by double integration of the corresponding EPR spectra. In the case of 1.75 mM TLR, the fraction of free TL1 (f_{free}) was determined to be 0.21 (Figure 5A). To quantitate the strength of the GAAA tetraloop/receptor interaction, f_{free} was measured for receptor concentrations in the range of 0.25−1.75 mM (Figure 6).

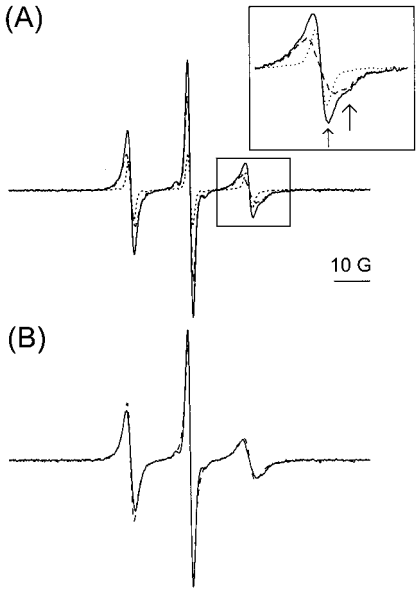

FIGURE 5: Dissecting the bound and free components. (A) Experimental EPR spectrum of spin labeled TL1 (~30 μM) in the presence of 1.75 mM TLR (solid trace) is shown, together with a scaled spectrum of spin labeled TL1 in the absence of receptor (representing the free TL1 in equilibrium with the complex, dotted trace), and the resulting difference spectrum (dashed trace) corresponding to the bound TL1 in the tetraloop/receptor complex. Buffer conditions are the same as those in Figure 4. Inset: The high-field portion of the spectrum is enlarged to reveal the free and bound components (indicated by arrows). (B) The difference spectrum (solid trace) was fitted (dashed trace) by a least-squares procedure using a program developed by Freed and co-workers (*40*). The principle values of *A* and *g* were set according to (*41*). The small satellites flanking the centerline arise from the natural abundance of ^{13}C and are not included in the program.

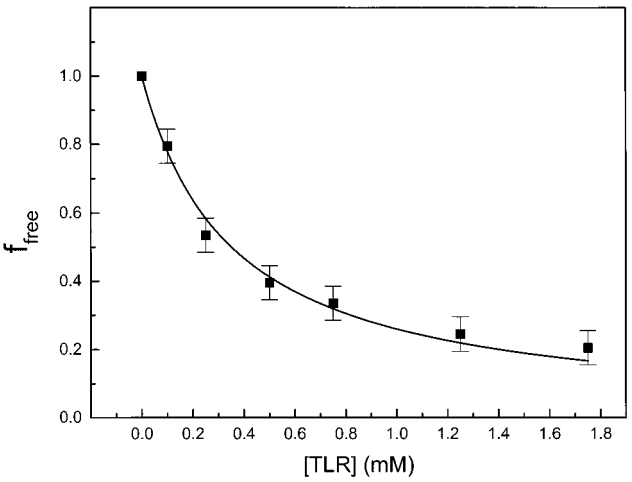

FIGURE 6: Determination of the K_d between the GAAA tetraloop and its receptor. The fraction of free population (f_{free}) was plotted against the concentration of the receptor. Buffer conditions are the same as those in Figure 4. Errors in the values of f_{free} were estimated to be ±0.05, which included errors from endpoint determinations in spectral titration, and propagated errors arising from integrations on which these fractions were based (*36*). K_d was determined according to eq 2 to be 0.40 ± 0.05 mM. The error in K_d was determined from two independent measurements.

The data were fit to an equation describing 1:1 binding (solid trace, Figure 6), and the dissociation constant, K_d, was determined to be 0.40 ± 0.05 mM, which corresponds to a binding energy, ΔG, of −4.6 kcal/mol.

Following the same procedure, the value of f_{free} was determined to be 0.67 for the interaction between the UUCG tetraloop hairpin (~30 μM) and 1.75 mM GAAA tetraloop receptor (Figure 4B, vide supra). This led to an estimated K_d of 3.6 mM, which is approximately an order of magnitude weaker than that of the GAAA tetraloop/receptor interaction and likely represents the nonspecific interactions.

Salt Dependence of the GAAA Tetraloop/Receptor Interaction. The data of Figure 6 were obtained in a buffer containing 125 mM $MgCl_2$ and 500 mM each of NaCl and KCl (Figure 6 legend). To investigate possible roles of the individual cations in the GAAA tetraloop/receptor interaction, the binding of labeled TL1 (≈30 μM) to 1.75 mM TLR was measured in 50 mM phosphate buffer (pH 6.0) containing either 125 mM $MgCl_2$, 500 mM NaCl, or 500mM KCl.

In the presence of 125 mM $MgCl_2$, addition of TLR to the labeled tetraloop caused a sharp reduction in amplitude of the high- and low-field resonance lines, indicating complex formation (Figure 7A). The value of f_{free} was determined to be 0.25, similar to that for the data in Figures 5 and 6 for the same receptor concentration. On the other hand, in the presence of 500 mM NaCl or KCl alone, the amplitude decrease was much less (Figure 7B,C), and values of f_{free} were found to be 0.60 and 0.68, respectively. Within experimental error, these values are the same as that measured for the UUCG tetraloop binding to the GAAA tetraloop receptor. These results indicate that Mg^{2+} is a major determinant for specific tetraloop/receptor interaction. Neither K^+ nor Na^+ alone is sufficient to support specific tetraloop/receptor interaction, although some weak, probably nonspecific, interaction cannot be ruled out.

The Mg^{2+} dependence was further analyzed by measuring tetraloop/receptor binding under various Mg^{2+} concentrations (Figure 8). As expected, f_{free} decreased as the concentration of Mg^{2+} increased. The data can be fit to a binding isotherm corresponding to the formation of a 1:1:1 complex of TL1, TLR, and Mg^{2+} (eq 3) with a K_{mg} of 39 ± 5.4 mM in the presence of TL1 (~30 μM) and 1.0 mM TLR.

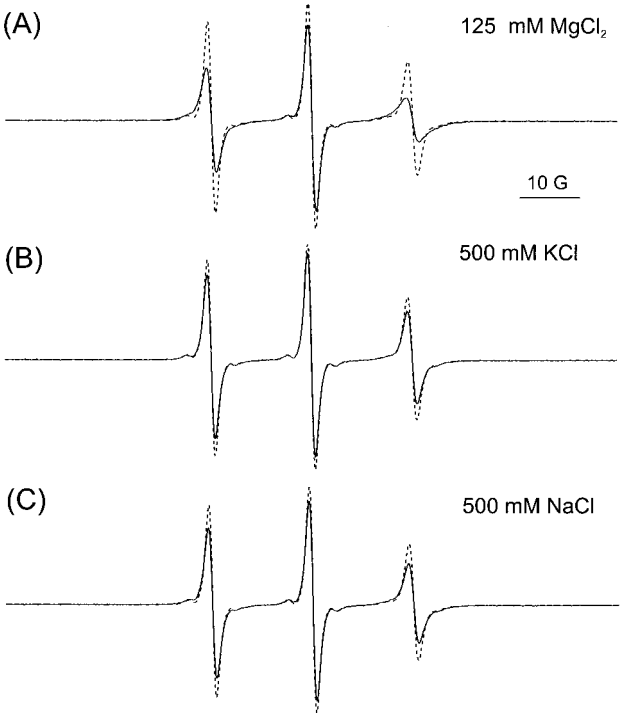

FIGURE 7: Salt dependence of the tetraloop/receptor interaction. Superimposed EPR spectra of labeled TL1 in the absence (dashed trace) and presence (solid trace) of 1.75 mM receptor in sodium phosphate buffer (50 mM, pH 6.0) containing (A) 125 mM $MgCl_2$, (B) 500 mM KCl, or (C) 500 mM NaCl.

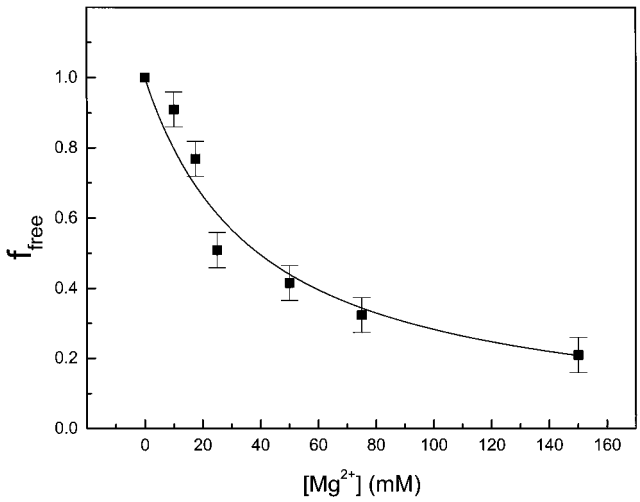

FIGURE 8: Mg^{2+} dependence of the isolated tetraloop/receptor interaction. Binding of labeled TL1 (~30 μM) to TLR (1 mM) was measured under various Mg^{2+} concentrations in the presence of MOPS buffer (50 mM, pH 6.6) containing 100 mM NaCl. Errors in the values of f_{free} were ±0.05 (see Figure 6 caption) (*36*). Fitting the data to eq 3 gave a K_{mg} = 39 ± 5.4 mM.

DISCUSSION

The Phosphorothioate Scheme for Site-Specific Labeling of RNA. One of the key issues in applying SDSL to RNA is the attachment of a proper nitroxide spin label at any desired location within the molecule of interest. Here, we present an efficient labeling scheme that allows one to place nitroxide labels at internal locations within RNA molecules (Figure 2). The method utilizes a universal backbone functionality of the RNA, and therefore is not restricted by the identity of the bases and is generally applicable to any RNA sequence. The position of the attachment site can be conveniently controlled during the chemical synthesis of RNA, thus allowing one to systematically scan the nitroxide label throughout the RNA molecule.

As is true for any method that utilizes external reporter groups, the degree of perturbation due to the extrinsic label has to be assessed. In the phosphorothioate labeling scheme, steric hindrance of the nitroxide moiety and loss of negative charges of the backbone will present perturbation around the labeling site. In addition, substitution of one of the nonbridging oxygens with sulfur and replacement of the 2′-OH group with a 2′-H might lead to loss of hydrogen binding and affect RNA tertiary contacts. In this work, thermal denaturation studies indicated that modification and labeling of the tetraloop hairpin near the 5′ terminus did not significantly disrupt the RNA secondary structure. However, the degree of perturbation is expected to vary from site to site, and may differ from system to system, and should be examined individually in specific studies.

While the phosphorothioate scheme provides a general method for internal spin labeling of RNA, chemical synthesis of the phosphorothioate creates two stereoisomers (*42*), which

might place the spin labels in slightly different environments. In this study, the existence of such isomers is not a problem, as the labeling site is not involved in the interaction under study and is used only as a sensor for the change of the global tumbling of the molecule. However, previous reports (*37*) and data presented here indicate that it is possible to separate the two isomers if required.

The phosphorothioate scheme was used previously for fluorophore labeling in RNA, although the efficiency of the labeling for internal phosphorothioates was not satisfactory (*29, 43*). Using a reactive α,β unsaturated iodo-methane derivative of a nitroxide (reagent **V**, Figure 2A), it is demonstrated here that the internal phosphorothioate sites can be efficiently modified. The same reactive function may be applicable for the attachment of other types of labels, such as fluorophores and photo-cross-linkers.

Recently, other methods for attaching nitroxide labels to RNA molecules have been reported: Variani and colleagues introduced 4-thiol U modifications as a labeling site for nitroxides (*25*); Shin and colleagues devised a 5′ displacement method to attach nitroxide labels to the 5′ terminus of RNA (*26*); and Sigurdsson and colleagues incorporated nitroxide spin labels at internal sites of the TAR RNA via 2′-amino modifications (*27*). Together with the phosphorothioate scheme presented here, a foundation has been set for the application of SDSL to study the structure and function of RNA.

Motion of the Nitroxide Spin Label Attached to the GAAA Tetraloop Hairpin. In the present study, the EPR spectra of the labeled tetraloop were analyzed in terms of a simple model in which contributions to the nitroxide rotational motion are treated as isotropic and independent. Two contributions are considered: overall rotational diffusion of the tetraloop (with correlation time τ_R), and internal rotations of the nitroxide due to torsional oscillations of bonds in the structure (with effective correlation time τ_i; see eq 4). The data presented above are internally consistent with this model. For example, the linearity of the $1/\tau$ vs $1/\eta$ plot (Figure 3) supports the assumption that the overall tumbling of the RNA hairpin is separable from internal modes that are apparently viscosity-independent. Moreover, the value estimated for τ_i (4.0 ± 1.6 ns) falls in the same range as that of the intrinsic motion of the same nitroxide side chain at an exposed site in T4 lysozyme ($\sim$3 ns) (*44*). Because the labeling site is far away from the tetraloop/receptor interface, the local environment of the nitroxide label should be invariant, and τ_i of the tetraloop/receptor complex should remain the same as that of the tetraloop alone. On the other hand, τ_R of the tetraloop/receptor complex should increase in proportion to the molecular weight, and $\tau_R^{complex} \approx 3\tau_R^{tetraloop} = 1.1$ ns. With this value and taking $\tau_i = 4$ ns, eq 4 can be used to estimate an overall $\tau = 0.9$ ns for nitroxide attached to the tetraloop/receptor complex. An independent value for τ may be estimated directly from the simulated spectrum of the complex (Figure 5B), where the geometric mean of the diffusion rates is $\langle R \rangle = \sqrt{R_{||}R_{\perp}} = 1.76 \times 10^8\ s^{-1}$, corresponding to a $<\tau>$ of 0.9 ns. Given the assumptions implicit in calculations of τ by these two approaches (especially the assumptions used to estimated $\tau_R^{complex}$), the agreement between the values is good, and supports the basic framework of the model employed to analyze the EPR spectra.

Because the motion of the labeled nitroxide is dominated by τ_R, the attached nitroxide is a sensitive molecular weight sensor and is able to reveal the formation of a weak complex. The location of the probe may be chosen so that it is far away from the interaction site to minimize the perturbation to the system under study. The EPR method requires a concentration of 20−100 μM of labeled sample, and can be generalized for measuring complex formation in the high micromolar to millimolar range.

The power of SDSL, however, extends beyond monitoring the overall tumbling of the molecule. From protein studies, it has been clearly demonstrated that the dynamics of the labeled nitroxide can be used to derive information on the secondary and tertiary structure (*20*−*23*). This is likely the case in RNA, although the exact correlation between the mobility of the nitroxide and the underlying RNA structure elements needs to be established (*27*). In addition, solvent accessibility and distance measurements are powerful tools that will yield a large amount of information on RNA structure and protein/RNA interactions (*25, 26*).

The GAAA Tetraloop/Receptor Interaction. The studies reported here reveal for the first time the formation of an isolated GAAA tetraloop/receptor complex in solution. The standard state interaction free energy was determined to be −4.6 kcal/mol with a saturating concentration of Mg^{2+} (125 mM). This value is comparable to results obtained with a variety of RNA constructs (*1*−*3, 8*−*14*). For example, in a recent study of RNA nano-structures engineered via the GAAA tetraloop/receptor motif, it was shown that a pair of well-organized GAAA tetraloop/receptors dimerizes with a ΔG of $\sim$−12 kcal/mol, while another less organized pair of GAAA tetraloop/receptors has ΔG of $\sim$−9 kcal/mol (*8*). These values correspond to −6 and −4.5 kcal/mol, respectively, for a single tetraloop/receptor interaction, similar to the value reported here. The differences may be due to the different experimental conditions, especially the different Mg^{2+} concentrations, and contributions from other tertiary interactions, including entropy effects.

The fact that Mg^{2+} is required for the tetraloop/receptor interaction is reasonable considering that Mg^{2+} ions are known to be directly involved in RNA tertiary structure formation (*45, 46*). The data presented here indicate that one specifically bound Mg^{2+} ion is involved in the GAAA tetraloop/receptor interaction (Figure 8), compatible with earlier reports (*8, 18*). In particular, the crystal structure of the tetraloop/receptor complex in the P46 domain of group I intron *Tetrahymena* reveals that one Mg^{2+} ion binds to the GAAA tetraloop receptor, making outer-sphere contacts with bases corresponding to A18, U19, and G20 of the receptor (*18*). Recently, a Mg^{2+} binding site within the GAAA tetraloop was also reported (*47, 48*). Whether or not the bound Mg^{2+} ion inferred from this study corresponds to one of these Mg^{2+} ions remains to be determined.

The apparent K_d for Mg^{2+} reported here (39 ± 5.4 mM) is similar to that for weak Mg^{2+} binding sites discovered in ribozyme constructs derived from group II introns and ribonuclease P RNAs (*49, 50*). However, it is around 50-fold higher than that reported for the tetraloop/receptor interaction embedded in various constructs derived from group I introns (*13, 51*). This difference is partially due to the entropy loss inherent in the bimolecular formation of the isolated tetraloop/receptor complex, and may well have

contributions due to the absence of additional RNA interactions in the isolated tetraloop/receptor complex. In this context, it is interesting to note that the Mg^{2+} ion revealed in the crystal structure of the tetraloop/receptor complex resides at the region where dramatic conformational rearrangement occurs (*17, 18*). If the Mg^{2+} ion shown in the crystal structure is indeed the Mg^{2+} ion detected in this work, it is possible that binding of Mg^{2+} is directly linked to receptor conformational changes, thus reducing the observed Mg^{2+} binding affinity. Such a scheme has been proposed previously (*50*), and further experiments are underway to test this hypothesis.

Neither Na^+ nor K^+ alone, even at very high ionic strength, promoted a significant level of tetraloop/receptor complex (Figure 7). A previous study reported that a K^+ ion binds specifically to the AA platform of the receptor and promotes folding of a larger RNA construct (*52*). In the present study, combining high concentrations of either Na^+ or K^+ with Mg^{2+} has a very limited effect in enhancing tetraloop/receptor binding. This difference raises the possibility that the configuration of the isolated tetraloop/receptor interaction observed here might be different from what is reported in previous work (*18*). SDSL studies are currently underway to obtain structural information on the isolated tetraloop/receptor complex in solution, and to directly study the resulting conformational changes as the tetraloop docks with the receptor.

ACKNOWLEDGMENT

We thank members of the Hubbell lab, especially Dr. C. Altenbach and L. Columbus, for their help. We also thank Dr. A. Pyle for helpful discussions and encouragement.

REFERENCES

1. Murphy, F. L., and Cech, T. R. (1994) *J. Mol. Biol. 236*, 49−63.
2. Jaeger, L., Michel, F., and Westhof, E. (1994) *J. Mol. Biol. 236*, 1271−1276.
3. Costa, M., and Michel, F. (1995) *EMBO J. 14*, 1276−1285.
4. Costa, M., and Michel, F. (1997) *EMBO J. 16*, 3289−3302.
5. Doudna, J. A. (2000) *Nat. Struct. Biol. Suppl.*, 954−956.
6. Conn, G. L., and Draper, D. E. (1998) *Curr. Opin. Struct. Biol. 8*, 278−285.
7. Ferre-d'Amare, A. R., Zhou, K., and Doudna, J. A. (1998) *J. Mol. Biol. 279*, 621−631.
8. Jaeger, L., and Leontis, N. B. (2000) *Angew. Chem., Int. Ed. Engl. 39*, 2521−2524.
9. Abramovitz, D. L., and Pyle, A. M. (1997) *J. Mol. Biol. 266*, 493−506.
10. Costa, M., Deme, E., Jacquier, A., and Michel, F. (1997) *J. Mol. Biol. 267*, 520−536.
11. Jestin, J. L., Deme, E., and Jacquier, A. (1997) *EMBO J. 16*, 2945−2954.
12. Massire, C., Jaeger, L., and Westhof, E. (1997) *RNA 3*, 553−556.
13. Doherty, E. A., Herschlag, D., and Doudna, J. A. (1999) *Biochemistry 38*, 2982−2990.
14. Ralston, C. Y., He, Q., Brenowitz, M., and Chance, M. R. (2000) *Nat. Struct. Biol. 7*, 371−374.
15. Tinoco, I., and Bustamante, C. (1999) *J. Mol. Biol. 293*, 271−281.
16. Jucker, F. M., Heus, H. A., Yip, P. F., Moors, E. H. M., and Pardi, A. (1996) *J. Mol. Biol. 264*, 968−980.
17. Butcher, S. E., Dieckmann, T., and Feigon, J. (1997) *EMBO J. 16*, 7490−7499.
18. Cate, J. H., Gooding, A. R., Podell, E., Zhou, K., Golden, B. L., Kundrot, C. E., Cech, T. R., and Doudna, J. A. (1996) *Science 273*, 1678−1685.
19. Pley, H. M., Flaherty, K. M., and McKay, D. B. (1994) *Nature 372*, 111−113.
20. Hubbell, W. L., and Altenbach, C. (1994) *Curr. Opin. Struct. Biol. 4*, 566−573.
21. Hubbell, W. L., Mchaourab, H. S., Altenbach, C., and Lietzow, M. A. (1996) *Structure 4*, 779−783.
22. Hubbell, W. L., Gross, A., Langen, R., and Leitzow, M. A. (1998) *Curr. Opin. Struct. Biol. 8*, 649−656.
23. Hubbell, W. L., Cafiso, D. S., and Altenbach, C. (2000) *Nat. Struct. Biol. 7*, 735−739.
24. Keyes, R. S., and Bobst, A. M. (1998) in *Biological Magnetic Resonance* (Berliner, L. J., Ed.) pp 283−338, Plenum Press, New York.
25. Ramos, A., and Varani, G. (1998) *J. Am. Chem. Soc. 120*, 10992−10993.
26. Macosko, J. C., Pio, M. S., Tinoco, I., Jr., and Shin, Y.-K. (1999) *RNA 5*, 1158−1166.
27. Edwards, T. E., Okonogi, T. M., Robinson, B. H., and Sigurdsson, S. T. (2001) *J. Am. Chem. Soc. 123*, 1527−1528.
28. Gish, G., and Eckstein, F. (1988) *Science 240*, 1520−1522.
29. Musier-Forsyth, K., and Schimmel, P. (1994) *Biochemistry 33*, 773−779.
30. Hankovszky, H. O., Heidge, K., and Lex, L. (1980) *Synthesis*, 914−916.
31. Hubbell, W. L., Froncisz, W., and Hyde, J. S. (1987) *Rev. Sci. Instrum. 58*, 1879−1886.
32. Knowles, P. F., Marsh, D., and Rattle, H. W. E. (1976) in *Magnetic Resonance of Biomolecules*, pp 168−207, John Wiley & Sons Ltd., New York.
33. Marsh, D. (1981) *Mol. Biol. Biochem. Biophys. 31*, 51−142.
34. Stone, T. J., Buckman, T., Nordio, P. L., and McConnell, H. M. (1965) *Proc. Natl. Acad. Sci. U.S.A. 54*, 1010−1017.
35. Bales, B. L. (1989) in *Biological Magnetic Resonance* (Berliner, L. J., and Reuben, J., Eds.) pp 77−130, Plenum Press, New York.
36. Jost, P. C., and Griffith, O. H. (1978) *Methods Enzymol. 49*, 369−418.
37. Slim, G., and Gait, M. J. (1991) *Nucleic Acids Res. 19*, 1183−1188.
38. Dudich, I. V., Timofeev, V. P., Vol'kenshtein, M. V., and Misharin, A. Y. (1977) *Mol. Biol. 11*, 685−693.
39. Mchaourab, H. S., Lietzow, M. A., Hideg, K., and Hubbell, W. L. (1996) *Biochemistry 35*, 7692−7704.
40. Budil, D. E., Lee, S., Saxena, S., and Freed, J. H. (1996) *J. Magn. Reson., Ser. A 120*, 155−189.
41. Columbus, L., Kalai, T., Jeko, J., Hideg, K., and Hubbell, W. L. (2001) *Biochemistry 40*, 3828−3846.
42. Eckstein, F. (1985) *Annu. Rev. Biochem. 54*, 367−402.
43. Qin, P. Z., and Pyle, A. M. (1999) *Methods 18*, 60−70.
44. Mchaourab, H. S., Kalai, T., Hideg, K., and Hubbell, W. L. (1999) *Biochemistry 38*, 2947−2955.
45. Pan, T., Long, D. M., and Ohlenbeck, O. C. (1993) in *The RNA world* (Gesteland, R. F., and Atkins, J. F., Eds.) pp 271−302, Cold Spring Harbor Laboratory Press, Plainview, NY.
46. Tinoco, I., and Kieft, J. S. (1997) *Nat. Struct. Biol. 4*, 509−512.
47. Rudisser, S., and Tinoco, I. (2000) *J. Mol. Biol. 295*, 1211−1223.
48. Maderia, M., Horton, T. E., and DeRose, V. J. (2000) *Biochemistry 39*, 8193−8200.
49. Beebe, J. A., Kurz, J. C., and Fierke, C. A. (1996) *Biochemistry 35*, 10493−10505.
50. Qin, P. Z., and Pyle, A. M. (1997) *Biochemistry 36*, 4718−4730.
51. Sclavi, B., Woodson, S., Sullivan, M., Chance, M. R., and Brenowitz, M. (1997) *J. Mol. Biol. 266*, 144−159.
52. Basu, S., Rambo, R. P., Strauss-Soukup, J., Cate, J. H., Ferre, D. A. A. R., Strobel, S. A., and Doudna, J. A. (1998) *Nat. Struct. Biol. 5*, 986−992.
53. *CRC Handbook of Biochemistry: Selected Data for Molecular Biology* (1970) 2nd ed., The Chemical Rubber Co., Cleveland, OH.

BI010294G